M02

Proceedings of the 5th International Conference on Inverse Problems in Engineering: Theory and Practice, Cambridge, UK, 11-15th July 2005

THE METHOD OF FUNDAMENTAL SOLUTIONS FOR SOLVING INVERSE BOUNDARY VALUE PROBLEMS IN ELASTICITY

L. MARIN
School of Mechanical, Materials, Manufacturing Engineering and Management, The University of Nottingham, Nottingham NG7 2RD, UK
E-mail: liviu.marin@nottingham.ac.uk

Abstract - The application of the method of fundamental solutions for solving inverse boundary value problems in two- and three-dimensional isotropic linear elasticity is investigated. The resulting system of linear algebraic equations is ill-conditioned and therefore its solution is regularized by employing the first-order Tikhonov functional, while the choice of the regularization parameter is based on the L-curve method. Numerical results are presented for both smooth and piecewise smooth geometries, as well as for constant and linear stress states. The convergence, accuracy and stability of the method with respect to increasing the number of source points and the distance between the source points and the boundary of the solution domain, and decreasing the amount of noise added into the input data, respectively, are analysed.

1. INTRODUCTION

The method of fundamental solutions (MFS) was originally introduced by Kupradze and Aleksidze [13], whilst its numerical formulation was first given by Mathon and Johnston [21]. The main idea of the MFS consists of approximating the solution of the problem by a linear combination of fundamental solutions with respect to some singularities/source points which are located outside the domain. Then, the original problem is reduced to determining the unknown coefficients of the fundamental solutions and the coordinates of the source points by requiring the approximation to satisfy the boundary conditions and hence solving a non-linear problem. If the source points are *a priori* fixed then the coefficients of the MFS approximation are determined by solving a linear problem. An excellent survey of the MFS and related methods over the past three decades has been presented in Fairweather and Karageorghis [3]. The advantages of the MFS over domain discretisation methods, such as the finite-difference method (FDM) and the finite element method (FEM), are very well documented [3]. In addition, the MFS has all the advantages of boundary methods, such as the boundary element method (BEM), as well as several advantages over other boundary methods. For example, the MFS does not require an elaborate discretisation of the boundary, integrations over the boundary are avoided, the solution in the interior of the domain is evaluated without extra quadratures, its implementation is very easy and only little data preparation is required. The most arguable issue regarding the MFS is still the location of the source points. However, this problem can be overcome by employing a non-linear least-squares minimisation procedure. Alternatively, the source points can be prescribed *a priori*, see [4], and the post-processing analysis of the errors can indicate their optimal location.

In most boundary value problems in solid mechanics, the governing system of partial differential equations, i.e. the equilibrium, constitutive and kinematics equations, has to be solved with the appropriate initial and boundary conditions for the displacement and/or traction vectors, i.e. Dirichlet, Neumann or mixed boundary conditions. These problems are called direct problems and their existence and uniqueness are well-established, see for example Knops and Payne [11]. However, there are other engineering problems which do not belong to this category. For example, when the material properties and/or the external sources are unknown, the geometry of a portion of the boundary is not determined or the boundary conditions are incomplete, either in the form of underspecified and overspecified boundary conditions on different parts of the boundary or the solution is prescribed at some internal points in the domain. These are inverse problems, and it is well known that they are generally ill-posed, i.e. the existence, uniqueness and stability of their solutions are not always guaranteed, see Hadamard [5].

A classical example of an inverse problem in elasticity is the Cauchy problem in which both displacement and traction boundary conditions are prescribed only on a part of the boundary of the solution domain, whilst no information is available on the remaining part of the boundary. This problem has been studied by many authors but only in the two-dimensional case. Maniatty *et al.* [15] have determined the traction boundary conditions by using a simple diagonal regularization in conjunction with the FEM. Spatial regularization, together with the BEM, has been used by Zabaras *et al.* [28] and with the FEM by Schnur and Zabaras [23]. Yeih *et al.* [27] have analysed its existence, uniqueness and continuous

dependence on the data and have proposed an alternative regularization procedure, namely the fictitious boundary indirect method, based on the simple or double layer potential theory. The numerical implementation of the aforementioned method has been undertaken by Koya *et al.* [12], who have used the BEM and the Nyström method for discretising the integrals. However, this formulation has not yet removed the problem of multiple integrations. Marin *et al.* [16] have determined the approximate solutions to the Cauchy problem in two-dimensional linear elasticity using an alternating iterative BEM which reduced the problem to solving a sequence of well-posed boundary value problems and they have later extended this numerical method to singular Cauchy problems, see Marin *et al.* [17]. Huang and Shih [9] and Marin *et al.* [18] have both used the conjugate gradient method combined with the BEM, in order to solve the same problem. The Tikhonov regularization method and the singular value decomposition, in conjunction with the BEM, have been employed by Marin and Lesnic [19, 20] to solve the two-dimensional Cauchy problem in linear elasticity.

In this study, we analyse the application of the MFS to solving the Cauchy problem in two- and three-dimensional isotropic linear elasticity. The MFS discretised system of equations is ill-conditioned and hence it is solved by employing the first-order Tikhonov regularization method, see e.g. Tikhonov and Arsenin [24], whilst the choice of the regularization parameter is based on the L-curve criterion, see Hansen [8]. Two benchmark examples for two- and three-dimensional isotropic linear elasticity involving smooth and piecewise smooth geometries are investigated. The convergence and stability of the method with respect to the location and the number of source points, and the amount of noise added into the Cauchy input data, respectively, are analysed.

2. MATHEMATICAL FORMULATION

Consider an isotropic linear elastic material which occupies an open bounded domain $\Omega \subset \mathbb{R}^d$, $d = 2, 3$, and assume that Ω is bounded by a piecewise smooth surface $\Gamma = \partial\Omega$, such that $\Gamma = \Gamma_1 \cup \Gamma_2$, where $\Gamma_1, \Gamma_2 \neq \emptyset$ and $\Gamma_1 \cap \Gamma_2 = \emptyset$. In the absence of body forces, the equilibrium equations with respect to the displacement vector $\boldsymbol{u}(\boldsymbol{x})$, also known as the Lamé or Navier equations, are given by, see e.g. Landau and Lifshits [14],

$$G\frac{\partial^2 u_i(\boldsymbol{x})}{\partial x_j \partial x_j} + \frac{G}{1-2\nu}\frac{\partial^2 u_j(\boldsymbol{x})}{\partial x_i \partial x_j} = 0, \qquad \boldsymbol{x} \in \Omega, \qquad i = 1, \ldots, d, \tag{1}$$

where G and ν are the shear modulus and Poisson ratio, respectively, and the customary standard Einstein notation for summation over repeated indices is used. The strains $\varepsilon_{ij}(\boldsymbol{x})$, $i, j = 1, \ldots, d$, are related to the displacement gradients by the kinematic relations

$$\varepsilon_{ij}(\boldsymbol{x}) = \frac{1}{2}\left(\frac{\partial u_i(\boldsymbol{x})}{\partial x_j} + \frac{\partial u_j(\boldsymbol{x})}{\partial x_i}\right), \qquad \boldsymbol{x} \in \overline{\Omega}, \qquad i, j = 1, \ldots, d, \tag{2}$$

while the stresses $\sigma_{ij}(\boldsymbol{x})$, $i, j = 1, \ldots, d$, are related to the strains through the constitutive law (Hooke's law), namely

$$\sigma_{ij}(\boldsymbol{x}) = 2G\left(\varepsilon_{ij}(\boldsymbol{x}) + \frac{\nu}{1-2\nu}\,\varepsilon_{kk}(\boldsymbol{x})\right), \qquad \boldsymbol{x} \in \overline{\Omega}, \qquad i, j = 1, \ldots, d, \tag{3}$$

with δ_{ij} the Kronecker delta tensor. We now let $\boldsymbol{n}(\boldsymbol{x})$ be the outward normal vector at Γ and $\boldsymbol{t}(\boldsymbol{x})$ be the traction vector at a point $\boldsymbol{x} \in \Gamma$ whose components are defined by

$$t_i(\boldsymbol{x}) = \sigma_{ij}(\boldsymbol{x})\; n_j(\boldsymbol{x}), \qquad \boldsymbol{x} \in \Gamma, \qquad i = 1, \ldots, d. \tag{4}$$

In the direct problem formulation, the knowledge of the displacement and/or traction vectors on the whole boundary Γ gives the corresponding Dirichlet, Neumann, or mixed boundary conditions which enables us to determine the displacement vector in the domain Ω. Then, the strain tensor ε_{ij} can be calculated from the kinematic relations (2) and the stress tensor is determined using the constitutive law (3). If it is possible to measure both the displacement and traction vectors on a part of the boundary Γ, say Γ_1, then this leads to the mathematical formulation of an inverse problem consisting of eqns. (1) and the boundary conditions

$$u_i(\boldsymbol{x}) = \widetilde{u}_i(\boldsymbol{x}), \qquad t_i(\boldsymbol{x}) = \widetilde{t}_i(\boldsymbol{x}), \qquad \boldsymbol{x} \in \Gamma_1, \qquad i = 1, \ldots, d, \tag{5}$$

where $\widetilde{\boldsymbol{u}}$ and $\widetilde{\boldsymbol{t}}$ are prescribed vector valued functions. In the above formulation of the boundary conditions (5), it can be seen that the boundary Γ_1 is overspecified by prescribing both the displacement

$\boldsymbol{u}|_{\Gamma_1} = \widetilde{\boldsymbol{u}}$ and the traction $\boldsymbol{t}|_{\Gamma_1} = \widetilde{\boldsymbol{t}}$ vectors, whilst the boundary Γ_2 is underspecified since both the displacement $\boldsymbol{u}|_{\Gamma_2}$ and the traction $\boldsymbol{t}|_{\Gamma_2}$ vectors are unknown and have to be determined. This problem, termed the Cauchy problem, is much more difficult to solve both analytically and numerically than the direct problem, since the solution does not satisfy the general conditions of well-posedness. Although the problem may have a unique solution, it is well known, see e.g. Hadamard [5], that this solution is unstable with respect to small perturbations in the data on Γ_1. Thus the problem is ill-posed and we cannot use a direct approach, such as the Gauss elimination method, in order to solve the system of linear equations which arises from the discretisation of the partial differential eqns. (1) and the boundary conditions (5). Therefore, regularization methods are required in order to solve accurately the Cauchy problem in linear elasticity.

3. THE METHOD OF FUNDAMENTAL SOLUTIONS

The fundamental solutions $\boldsymbol{U}^{(k)}$, $k = 1, \ldots, d$, of the Lamé system (1) in the two- ($d = 2$) and three-dimensional ($d = 3$) cases are given by, see e.g. Berger and Karageorghis [1] and Poullikkas *et al.* [22],

$$\boldsymbol{U}^{(k)}(\boldsymbol{x}, \boldsymbol{y}) = \sum_{i=1}^{d} U_{ik}(\boldsymbol{x}, \boldsymbol{y})\, \boldsymbol{e}_i, \qquad \boldsymbol{x} \in \overline{\Omega}, \qquad \boldsymbol{y} \in \mathbb{R}^d \setminus \overline{\Omega}, \qquad k = 1, \ldots d, \tag{6}$$

where $\boldsymbol{y}$ is a source point, $\boldsymbol{e}_i$, $i = 1, \ldots, d$, is the unit vector along the x_i-axis and

$$U_{ik}(\boldsymbol{x}, \boldsymbol{y}) = \begin{cases} -\dfrac{1}{8\pi G(1-\overline{\nu})} \left((3 - 4\overline{\nu}) \ln r(\boldsymbol{x}, \boldsymbol{y})\ \delta_{ik} - \dfrac{(x_i - y_i)(x_k - x_k)}{r^2(\boldsymbol{x}, \boldsymbol{y})} \right), & d = 2 \\ \dfrac{1}{16\pi G(1-\nu)} \dfrac{1}{r(\boldsymbol{x}, \boldsymbol{y})} \left((3 - 4\nu)\ \delta_{ik} + \dfrac{(x_i - y_i)(x_k - x_k)}{r^2(\boldsymbol{x}, \boldsymbol{y})} \right), & d = 3 \end{cases} \tag{7}$$

Here $r^2(\boldsymbol{x}, \boldsymbol{y}) = \sum_{i=1}^{d} (x_i - y_i)^2$ represents the distance between the domain point $\boldsymbol{x} = (x_1, \ldots, x_d)$ and the source point $\boldsymbol{y} = (y_1, \ldots, y_d)$, δ_{ik} is the Kronecker delta tensor, and $\overline{\nu} = \nu$ in the plane strain state and $\overline{\nu} = \nu/(1+\nu)$ in the plane stress state for $d = 2$.

Justified by a density result, see Bogomolny [2], the main idea of the MFS consists of the approximation of the displacement vector in the solution domain by a linear combination of fundamental solutions with respect to M source points $\boldsymbol{y}_j \in \mathbb{R}^d \setminus \overline{\Omega}$ in the form

$$\boldsymbol{u}(\boldsymbol{x}) \approx \boldsymbol{u}^M \left(\boldsymbol{a}^{(1)}, \ldots, \boldsymbol{a}^{(d)}, \boldsymbol{Y}; \boldsymbol{x} \right) = \sum_{j=1}^{M} \sum_{k=1}^{d} a_j^{(k)} \boldsymbol{U}^{(k)}\left(\boldsymbol{x}, \boldsymbol{y}^j\right), \qquad \boldsymbol{x} \in \overline{\Omega}, \tag{8}$$

where $\boldsymbol{a}^{(k)} = \left(a_1^{(k)}, \ldots, a_M^{(k)} \right)$, $k = 1, \ldots, d$, and $\boldsymbol{Y}$ is a $(dM)-$vector containing the coordinates of the source points $\boldsymbol{y}^j$, $j = 1, \ldots, M$. On taking into account the kinematic relations (2), the constitutive law (3), the definitions of the components of the traction vector (4) and the fundamental solutions (6) then the traction vector can be approximated on the boundary Γ by

$$\boldsymbol{t}^M \left(\boldsymbol{a}^{(1)}, \ldots, \boldsymbol{a}^{(d)}, \boldsymbol{Y}; \boldsymbol{x}, \boldsymbol{n}(\boldsymbol{x}) \right) = \sum_{j=1}^{M} \sum_{k=1}^{d} a_j^{(k)} \boldsymbol{T}^{(k)}\left(\boldsymbol{x}, \boldsymbol{y}^j; \boldsymbol{n}(\boldsymbol{x})\right), \qquad \boldsymbol{x} \in \Gamma, \tag{9}$$

where

$$\boldsymbol{T}^{(k)}(\boldsymbol{x}, \boldsymbol{y}) = \sum_{i=1}^{d} T_{ik}(\boldsymbol{x}, \boldsymbol{y}; \boldsymbol{n}(\boldsymbol{x}))\, \boldsymbol{e}_i, \qquad \boldsymbol{x} \in \Gamma, \qquad \boldsymbol{y} \in \mathbb{R}^d \setminus \overline{\Omega}, \qquad k = 1, \ldots, d. \tag{10}$$

Here the functions $T_{ik}(\boldsymbol{x}, \boldsymbol{y}; \boldsymbol{n}(\boldsymbol{x}))$, $i, k = 1, \ldots, d$, are given by the following expressions:

$$\begin{aligned} T_{1k}(\boldsymbol{x}, \boldsymbol{y}; \boldsymbol{n}(\boldsymbol{x})) &= 2G \left(\frac{1-\overline{\nu}}{1-2\overline{\nu}} \frac{\partial U_{1k}(\boldsymbol{x}, \boldsymbol{y})}{\partial x_1} + \frac{\overline{\nu}}{1-2\overline{\nu}} \frac{\partial U_{2k}(\boldsymbol{x}, \boldsymbol{y})}{\partial x_2} \right) n_1(\boldsymbol{x}) \\ &\quad + G \left(\frac{\partial U_{1k}(\boldsymbol{x}, \boldsymbol{y})}{\partial x_2} + \frac{\partial U_{2k}(\boldsymbol{x}, \boldsymbol{y})}{\partial x_1} \right) n_2(\boldsymbol{x}), \qquad k = 1, 2, \\ T_{2k}(\boldsymbol{x}, \boldsymbol{y}; \boldsymbol{n}(\boldsymbol{x})) &= G \left(\frac{\partial U_{1k}(\boldsymbol{x}, \boldsymbol{y})}{\partial x_2} + \frac{\partial U_{2k}(\boldsymbol{x}, \boldsymbol{y})}{\partial x_1} \right) n_1(\boldsymbol{x}) \\ &\quad + 2G \left(\frac{\overline{\nu}}{1-2\overline{\nu}} \frac{\partial U_{1k}(\boldsymbol{x}, \boldsymbol{y})}{\partial x_1} + \frac{1-\overline{\nu}}{1-2\overline{\nu}} \frac{\partial U_{2k}(\boldsymbol{x}, \boldsymbol{y})}{\partial x_2} \right) n_2(\boldsymbol{x}), \qquad k = 1, 2, \end{aligned} \tag{11}$$

and

$$
\begin{aligned}
T_{1k}\left(\boldsymbol{x},\boldsymbol{y};\boldsymbol{n}(\boldsymbol{x})\right) &= \frac{2G}{1-2\nu}\left((1-\nu)\frac{\partial U_{1k}(\boldsymbol{x},\boldsymbol{y})}{\partial x_1}+\nu\frac{\partial U_{2k}(\boldsymbol{x},\boldsymbol{y})}{\partial x_2}+\nu\frac{\partial U_{3k}(\boldsymbol{x},\boldsymbol{y})}{\partial x_3}\right)n_1(\boldsymbol{x})\\
&+G\left(\frac{\partial U_{1k}(\boldsymbol{x},\boldsymbol{y})}{\partial x_2}+\frac{\partial U_{2k}(\boldsymbol{x},\boldsymbol{y})}{\partial x_1}\right)n_2(\boldsymbol{x})+G\left(\frac{\partial U_{1k}(\boldsymbol{x},\boldsymbol{y})}{\partial x_3}+\frac{\partial U_{3k}(\boldsymbol{x},\boldsymbol{y})}{\partial x_1}\right)n_3(\boldsymbol{x}),\ k=1,2,3,\\
T_{2k}\left(\boldsymbol{x},\boldsymbol{y};\boldsymbol{n}(\boldsymbol{x})\right) &= \frac{2G}{1-2\nu}\left(\nu\frac{\partial U_{1k}(\boldsymbol{x},\boldsymbol{y})}{\partial x_1}+(1-\nu)\frac{\partial U_{2k}(\boldsymbol{x},\boldsymbol{y})}{\partial x_2}+\nu\frac{\partial U_{3k}(\boldsymbol{x},\boldsymbol{y})}{\partial x_3}\right)n_2(\boldsymbol{x})\\
&+G\left(\frac{\partial U_{2k}(\boldsymbol{x},\boldsymbol{y})}{\partial x_3}+\frac{\partial U_{3k}(\boldsymbol{x},\boldsymbol{y})}{\partial x_2}\right)n_3(\boldsymbol{x})+G\left(\frac{\partial U_{2k}(\boldsymbol{x},\boldsymbol{y})}{\partial x_1}+\frac{\partial U_{1k}(\boldsymbol{x},\boldsymbol{y})}{\partial x_2}\right)n_1(\boldsymbol{x}),\ k=1,2,3,\\
T_{3k}\left(\boldsymbol{x},\boldsymbol{y};\boldsymbol{n}(\boldsymbol{x})\right) &= \frac{2G}{1-2\nu}\left(\nu\frac{\partial U_{1k}(\boldsymbol{x},\boldsymbol{y})}{\partial x_1}+\nu\frac{\partial U_{2k}(\boldsymbol{x},\boldsymbol{y})}{\partial x_2}+(1-\nu)\frac{\partial U_{3k}(\boldsymbol{x},\boldsymbol{y})}{\partial x_3}\right)n_3(\boldsymbol{x})\\
&+G\left(\frac{\partial U_{3k}(\boldsymbol{x},\boldsymbol{y})}{\partial x_1}+\frac{\partial U_{1k}(\boldsymbol{x},\boldsymbol{y})}{\partial x_3}\right)n_1(\boldsymbol{x})+G\left(\frac{\partial U_{3k}(\boldsymbol{x},\boldsymbol{y})}{\partial x_2}+\frac{\partial U_{2k}(\boldsymbol{x},\boldsymbol{y})}{\partial x_3}\right)n_2(\boldsymbol{x}),\ k=1,2,3,
\end{aligned}
\tag{12}
$$

for two- and three-dimensions, respectively.

If N collocation points $\boldsymbol{x}^i$, $i=1,\ldots,N$, are chosen on the overspecified boundary Γ_1 and the locations of the source points $\boldsymbol{y}^j$, $j=1,\ldots,M$, are set in $\mathbb{R}^d\setminus\overline{\Omega}$ then eqns. (5), (8) and (9) generate a system of $(2dN)$ linear algebraic equations with (dM) unknowns which can be generically written as

$$
\mathbb{A}\boldsymbol{X}=\boldsymbol{F},
\tag{13}
$$

where the MFS matrix $\mathbb{A}\in\mathbb{R}^{2dN\times dM}$, the unknown vector $\boldsymbol{X}\in\mathbb{R}^{dM}$ and the right-hand side vector $\boldsymbol{F}\in\mathbb{R}^{2dN}$ are given by

$$
\begin{array}{lll}
A_{(k-1)N+i,\ (l-1)M+j}=U_{kl}\left(\boldsymbol{x}^i,\boldsymbol{y}^j\right), & A_{(k+d-1)N+i,\ (l-1)M+j}=T_{kl}\left(\boldsymbol{x}^i,\boldsymbol{y}^j\right), & X_{(k-1)M+j}=a_j^{(k)},\\
F_{(k-1)N+i}=\widetilde{u}_k\left(\boldsymbol{x}^i\right), & F_{(k+d-1)N+i}=\widetilde{t}_k\left(\boldsymbol{x}^i\right), & \\
i=1,\ldots,N, & j=1,\ldots,M, & k,l=1,\ldots,d.
\end{array}
\tag{14}
$$

It should be noted that in order to uniquely determine the solution $\boldsymbol{X}$ of the system of linear algebraic eqns. (13), i.e. the coefficients $a_j^{(k)}$, $j=1,\ldots,M$, $k=1,\ldots,d$, in the approximations (8) and (9), the number N of boundary collocation points and the number M of source points must satisfy the inequality $M\leq 2N$. However, the system of linear algebraic eqns. (13) cannot be solved by direct methods, such as the least-squares method, since such an approach would produce a highly unstable solution. Most of the standard numerical methods cannot achieve a good accuracy in the solution of the system of linear algebraic eqns. (13) due to the large value of the condition number of the matrix $\mathbb{A}$ which increases dramatically as the number of boundary collocation points and source points increases. It should be mentioned that for inverse problems, the resulting systems of linear algebraic equations are ill-conditioned, even if other well-known numerical methods (FDM, FEM or BEM) are employed.

4. THE TIKHONOV REGULARIZATION METHOD

Several regularization procedures have been developed to solve such ill-conditioned problems, see for example Hansen [7]. However, we only consider the Tikhonov regularization method, see Tikhonov and Arsenin [24], in our study since it is simple, non-iterative and it provides an explicit solution, see eqn. (17) below. Furthermore, the Tikhonov regularization method is feasible to apply for large systems of equations unlike the singular value decomposition which may become prohibitive for such large problems, see Hansen [8].

The Tikhonov regularized solution to the system of linear algebraic eqns. (13) is sought as

$$
\boldsymbol{X}_\lambda:\mathcal{T}_\lambda(\boldsymbol{X}_\lambda)=\min_{\boldsymbol{X}\in\mathbb{R}^{dM}}\mathcal{T}_\lambda(\boldsymbol{X}),
\tag{15}
$$

where $\mathcal{T}_\lambda$ represents the $k-$th order Tikhonov functional given by

$$
\mathcal{T}_\lambda(\cdot):\mathbb{R}^{dM}\longrightarrow[0,\infty),\qquad \mathcal{T}_\lambda(\boldsymbol{X})=||\mathbb{A}\boldsymbol{X}-\boldsymbol{F}||_2^2+\lambda^2||\mathbb{R}^{(k)}\boldsymbol{X}||_2^2,
\tag{16}
$$

the matrix $\mathbb{R}^{(k)}\in\mathbb{R}^{(dM-k)\times dM}$ induces a $\mathcal{C}^k-$constraint on the solution $\boldsymbol{X}$ and $\lambda>0$ is the regularization parameter to be chosen. Formally, the Tikhonov regularized solution $\boldsymbol{X}_\lambda$ of the problem (15) is given as the solution of the regularized equation

$$
\left(\mathbb{A}^T\mathbb{A}+\lambda^2{\mathbb{R}^{(k)}}^T\mathbb{R}^{(k)}\right)\boldsymbol{X}=\mathbb{A}^T\boldsymbol{F}.
\tag{17}
$$

Regularization is necessary when solving ill-conditioned systems of linear equations because the simple least-squares solution, i.e. $\lambda = 0$, is completely dominated by contributions from data errors and rounding errors. By adding regularization we are able to damp out these contributions and maintain the norm $||\mathbb{R}^{(k)}\boldsymbol{X}||_2$ to be of reasonable size.

The choice of the regularization parameter in eqn. (17) is crucial for obtaining a stable solution and this is discussed next. If too much regularization, or damping, i.e. λ^2 is large, is imposed on the solution of eqn. (17) then it will not fit the given data $\boldsymbol{F}$ properly and the residual norm $||\mathbb{A}\boldsymbol{X} - \boldsymbol{F}||_2$ will be too large. If too little regularization is imposed on the solution of eqn. (17), i.e. λ^2 is small, then the fit will be good, but the solution will be dominated by the contributions from the data errors, and hence $||\mathbb{R}^{(k)}\boldsymbol{X}||_2$ will be too large. It is quite natural to plot the norm of the solution as a function of the norm of the residual parametrised by the regularization parameter λ, i.e. $\big\{\big(||\mathbb{A}\boldsymbol{X}_\lambda - \boldsymbol{F}||_2, ||\mathbb{R}^{(k)}\boldsymbol{X}_\lambda||_2\big) \mid \lambda > 0\big\}$. Hence, the L-curve is really a trade-off curve between two quantities that both should be controlled and, according to the L-curve criterion, the optimal value λ_{opt} of the regularization parameter λ is chosen at the "corner" of the L-curve, see Hansen [7, 8].

As with every practical method, the L-curve has its advantages and disadvantages. There are two main disadvantages or limitations of the L-curve criterion. The first disadvantage is concerned with the reconstruction of very smooth exact solutions, see Tikhonov *et al.* [25]. For such solutions, Hanke [6] showed that the L-curve criterion will fail, and the smoother the solution, the worse the regularization parameter λ computed by the L-curve criterion. However, it is not clear how often very smooth solutions arise in applications. The second limitation of the L-curve criterion is related to its asymptotic behaviour as the problem size dM increases. As pointed out by Vogel [26], the regularization parameter λ computed by the L-curve criterion may not behave consistently with the optimal parameter λ_{opt} as dM increases. However, this ideal situation in which the same problem is discretised for increasing dM may not arise so often in practice. Often the problem size dM is fixed by the particular measurement setup given by $2dN$, and if a larger dM is required then a new experiment must be undertaken since the inequality $M \leq 2N$ must be satisfied. Apart from these two limitations, the advantages of the L-curve criterion are its robustness and ability to treat perturbations consisting of correlated noise, see for more details Hansen [8].

5. NUMERICAL RESULTS AND DISCUSSION

Although neither convergence nor estimate proofs are as yet available for the MFS applied to linear elasticity, the numerical results presented in this section for the Cauchy problem in two- and three-dimensional isotropic linear elasticity indicate that the proposed method is feasible and efficient. In order to present the performance of the MFS in conjunction with the first-order Tikhonov regularization method, we consider an isotropic linear elastic medium characterised by the material constants $G = 3.35 \times 10^{10}$ N/m^2 and $\nu = 0.34$ corresponding to a copper alloy and we solve the Cauchy problem (1) and (5) for two typical examples in a smooth two-dimensional geometry and a piecewise smooth three-dimensional domain:

Example 1. We consider the following analytical solution for the displacements:

$$u_i^{(\text{an})}(x_1, x_2) = \frac{1-\nu}{2G(1+\nu)}\sigma_0 x_i, \qquad i = 1, 2, \qquad \sigma_0 = 1.5 \times 10^{10} \text{ N/m}^2, \tag{18}$$

in the unit disk $\Omega = \big\{\boldsymbol{x} = (x_1, x_2) \;\big|\; x_1^2 + x_2^2 < 1\big\} \subset \mathbb{R}^2$, which corresponds to a uniform hydrostatic stress given by

$$\sigma_{ij}^{(\text{an})}(x_1, x_2) = \sigma_0 \delta_{ij}, \qquad i, j = 1, 2. \tag{19}$$

Here $\Gamma_1 = \big\{\boldsymbol{x} \in \Gamma \;\big|\; 0 \leq \theta(\boldsymbol{x}) \leq \pi/4\big\}$ and $\Gamma_2 = \big\{\boldsymbol{x} \in \Gamma \;\big|\; \pi/4 < \theta(\boldsymbol{x}) < 2\pi\big\}$, where $\theta(\boldsymbol{x})$ is the angular polar coordinate of $\boldsymbol{x}$.

Example 2. We consider the following analytical solution for the displacements:

$$u_i^{(\text{an})}(\boldsymbol{x}) = x_i, \qquad i = 1, 2, 3, \tag{20}$$

in the domain $\Omega = (-0.5, 0.5)^3 \subset \mathbb{R}^3$, which corresponds to a uniform hydrostatic stress given by

$$\sigma_{ij}^{(\text{an})}(\boldsymbol{x}) = \frac{2G(1+\nu)}{1-2\nu}\delta_{ij}, \qquad i, j = 1, 2, 3. \tag{21}$$

Here $\Gamma_1 = \bigcup_{j=1}^{5} \Gamma^{(j)}$ and $\Gamma_2 = \Gamma \setminus \Gamma_1 = \Gamma^{(6)}$, where $\Gamma = \bigcup_{j=1}^{6} \Gamma^{(j)}$, $\Gamma^{(j)} = \{\boldsymbol{x} \in \Gamma \mid x_j = -0.5\}$, $j = 1, 2, 3$, and $\Gamma^{(j+3)} = \{\boldsymbol{x} \in \Gamma \mid x_j = 0.5\}$, $j = 1, 2, 3$.

It should be noted that for the examples considered, the Cauchy data is available on a portion Γ_1 of the boundary Γ such that $\text{meas}(\Gamma_1) = \text{meas}(\Gamma)/4$ in the case of Example 1 and $\text{meas}(\Gamma_1) = 5\,\text{meas}(\Gamma)/6$ in the case of Example 2. The Cauchy problems investigated in this study have been solved using a uniform distribution of both the boundary collocation points $\boldsymbol{x}^i$, $i = 1, \ldots, N$, and the source points $\boldsymbol{y}^j$, $j = 1, \ldots, M$. The latter were located on the boundary of the disk $\text{B}(0, R) \subset \mathbb{R}^2$, where the radius $R > 1.0$ was chosen such that $\overline{\Omega} \subset \text{B}(0, R)$ in the case of Example 1 and on the boundary of the cube $\widetilde{\Omega} = (-R, R)^3 \subset \mathbb{R}^3$, where $R > 0.5$ was chosen such that $\overline{\Omega} \subset \widetilde{\Omega}$ in the case of Example 2. Furthermore, the number of boundary collocation points was set to $N = 40$ for the Example 1 and $N = 600$ for the Example 2.

5.1. Stability of the method

In order to investigate the stability of the MFS, the displacement vector $\boldsymbol{u}|_{\Gamma_1} = \boldsymbol{u}^{(\text{an})}|_{\Gamma_1}$ has been perturbed as

$$\widetilde{u}_i = u_i + \delta u_i, \qquad i = 1, \ldots, d, \tag{22}$$

where δu_i is a Gaussian random variable with mean zero and standard deviation $\sigma_i = \max_{\Gamma_1} |u_i| \; (p_u/100)$, generated by the NAG subroutine G05DDF, and $p_u\%$ is the percentage of additive noise included in the input data $\boldsymbol{u}|_{\Gamma_1}$ in order to simulate the inherent measurement errors.

Figure 1(a) presents the L-curves obtained for the Cauchy problem given by Example 1 using the

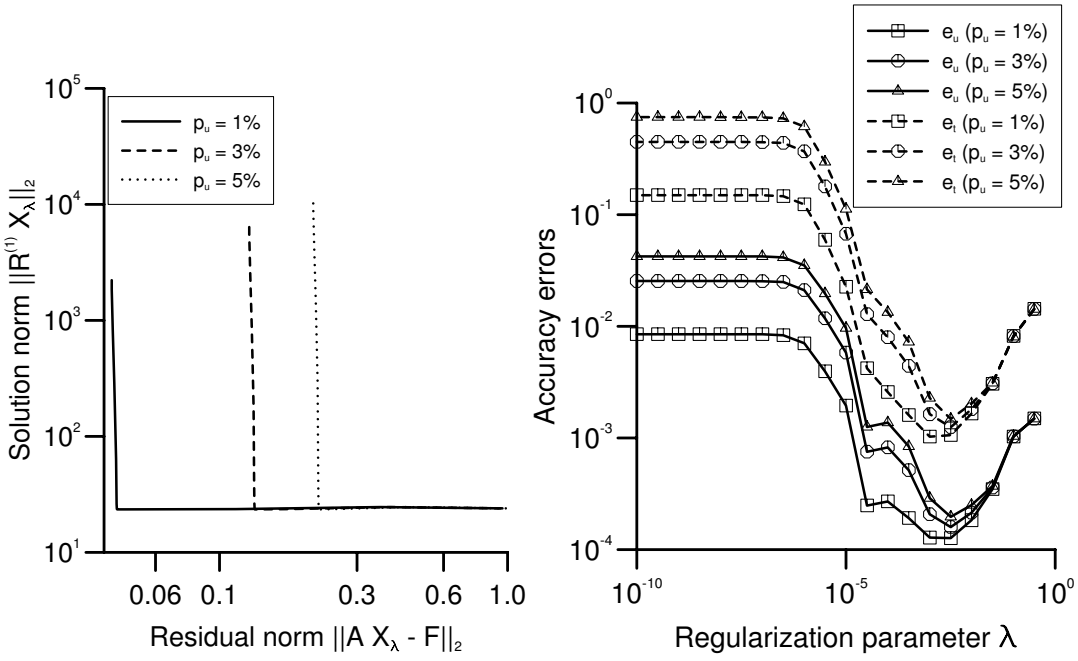

(a) (b)

Figure 1: (a) The L-curves obtained for various levels of noise added into the displacement data $\boldsymbol{u}|_{\Gamma_1}$, namely $p_u = 1\%$ (——), $p_u = 3\%$ (− −) and $p_u = 5\%$ (· · ·), and (b) the accuracy errors e_u (——) and e_t (− −) as functions of the regularization parameter λ, obtained for various levels of noise added into the displacement $\boldsymbol{u}|_{\Gamma_1}$, namely $p_u = 1\%$ (□), $p_u = 3\%$ (◯) and $p_u = 5\%$ (△), with $M = 10$ source points, $N = 40$ boundary collocation points and $R = 5.0$ for the Example 1.

first-order Tikhonov regularization method, i.e. $k = 1$ in (16), to solve the MFS system of eqns. (13), $M = 10$ source points, $R = 5.0$ and with various levels of noise added into the input displacement data. From this figure it can be seen that for each amount of noise considered the "corner" of the corresponding L-curve can be clearly determined and $\lambda = \lambda_{\text{opt}} = 1.0 \times 10^{-3}$ and $\lambda = \lambda_{\text{opt}} = 3.16 \times 10^{-3}$ for $p_u = 1$ and $p_u \in \{3, 5\}$, respectively.

In order to analyse the accuracy of the numerical results obtained, we introduce the errors e_u and e_t given by

$$e_u(\lambda) = \sqrt{\frac{1}{L}\sum_{l=1}^{L}\left(\boldsymbol{u}^{(\mathrm{an})}\left(\boldsymbol{x}^l\right) - \boldsymbol{u}^{(\lambda)}\left(\boldsymbol{x}^l\right)\right)^2}, \qquad e_t(\lambda) = \frac{1}{10^{10}}\sqrt{\frac{1}{L}\sum_{l=1}^{L}\left(\boldsymbol{t}^{(\mathrm{an})}\left(\boldsymbol{x}^l\right) - \boldsymbol{t}^{(\lambda)}\left(\boldsymbol{x}^l\right)\right)^2}, \quad (23)$$

where $\boldsymbol{x}^l$, $l = 1, \ldots, L$, are L uniformly distributed points on the underspecified boundary Γ_2, $\boldsymbol{u}^{(\mathrm{an})}$ and $\boldsymbol{t}^{(\mathrm{an})}$ are the analytical displacement and traction vectors, respectively, and $\boldsymbol{u}^{(\lambda)}$ and $\boldsymbol{t}^{(\lambda)}$ are the numerical displacement and traction vectors, respectively, obtained for the value λ of the regularization parameter. Figure 1(b) illustrates the accuracy errors e_u and e_t given by relation (23), as functions of the regularization parameter λ, obtained with various levels of noise added into the input displacement data $\boldsymbol{u}|_{\Gamma_1}$ for the Cauchy problem given by Example 1. From this figure it can be seen that both errors e_u and e_t decrease as the level of noise added into the input displacement data decreases for all the regularization parameters λ and $e_u < e_t$ for all the regularization parameters λ and a fixed amount p_u of noise added into the input displacement data, i.e. the numerical results obtained for the displacements are more accurate than those retrieved for the tractions on the underspecified boundary Γ_2. Furthermore, by comparing Figures 1(a) and (b), it can be seen, for various levels of noise, that the "corner" of the L-curve occurs at about the same value of the regularization parameter λ where the minimum in the accuracy errors e_u and e_t is attained. Hence the choice of the optimal regularization parameter λ_{opt} according to the L-curve criterion is fully justified. Similar results have been obtained for the Cauchy problem given by Example 2 and therefore they are not presented here.

Figures 2(a) and (b) illustrate the analytical and the numerical results for the displacement u_1 and

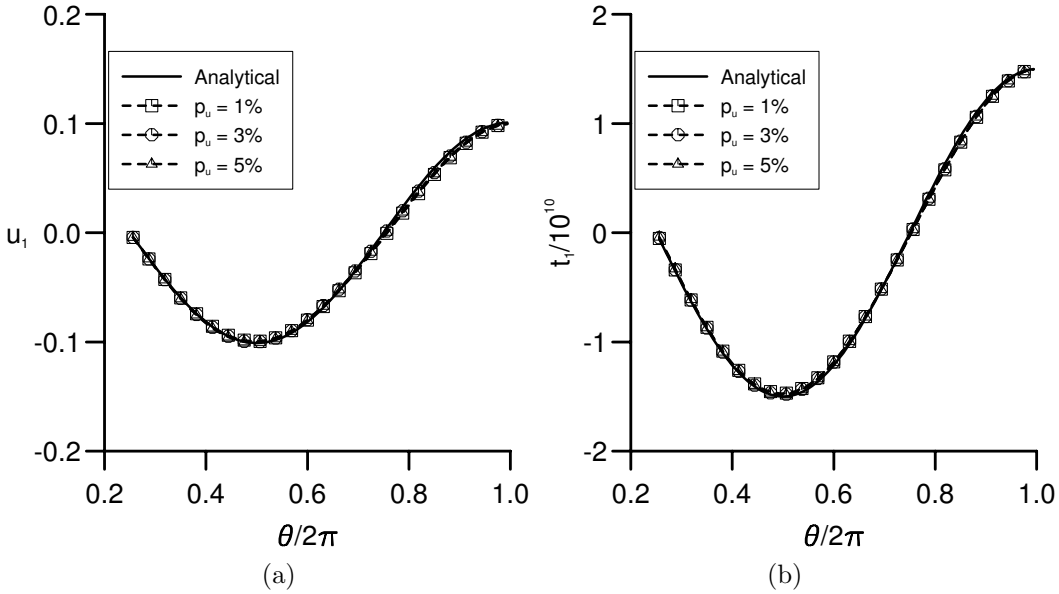

Figure 2: (a) The analytical $u_1^{(\mathrm{an})}$ (——) and the numerical $u_1^{(\lambda)}$ displacements, and (b) the analytical $t_2^{(\mathrm{an})}$ (——) and the numerical $t_2^{(\lambda)}$ tractions, retrieved on the underspecified boundary Γ_2 with $M = 10$ source points, $N = 40$ boundary collocation points, $R = 5.0$, $\lambda = \lambda_{\mathrm{opt}}$ and various levels of noise added into the displacement $\boldsymbol{u}|_{\Gamma_1}$, namely $p_u = 1\%$ ($-\square-$), $p_u = 3\%$ ($-\bigcirc-$) and $p_u = 5\%$ ($-\triangle-$), for the Example 1.

the traction t_2, respectively, obtained on the underspecified boundary Γ_2 using the optimal regularization parameter $\lambda = \lambda_{\mathrm{opt}}$ chosen according to the L-curve criterion, $M = 10$ source points, $R = 5.0$ and various levels of noise added into the input displacement data $\boldsymbol{u}|_{\Gamma_1}$, namely $p_u \in \{1, 3, 5\}$, for the Cauchy problem given by Example 1. From these figures we can conclude that the numerical solutions retrieved for Example 1 are stable with respect to the amount of noise p_u added into the input diplacement data $\boldsymbol{u}|_{\Gamma_1}$. Although not presented here, it is reported that a similar conclusion can be drawn from the numerical results obtained for the Cauchy problem given by Example 2.

5.2. Convergence and accuracy of the method

Although not illustrated, it is reported that the convergence of the numerical solutions for the displacement and the traction vectors on the underspecified boundary Γ_2 towards their analytical solutions, respectively, as M or R increases, has been obtained when $p_u = 0$ for both examples considered in this study. In order to investigate the influence of the number M of source points on the accuracy and stability of the numerical solutions for the displacement and the traction vectors on the underspecified boundary Γ_2, we set $R = 5.0$ and $p_u = 5$ for the Cauchy problem given by Example 2. In Figures 3(a) and (b) we present the accuracy errors e_u and e_t, respectively, as functions of the number M of source points, obtained using the optimal values of $\lambda = \lambda_{\text{opt}}$ given by the L-curve criterion for each value of M. It can be seen from these figures that both accuracy errors tend to zero as the number M of source points increases and, in addition, these errors do not decrease substantially for $M \geq 54$. These results indicate the fact that accurate numerical solutions for the displacement and the traction vectors on the underspecified boundary Γ_2 can be obtained using a relatively small number M of source points. Similar results have been obtained for the Cauchy problem given by Example 1 and therefore they are not presented here. From Figures 3(a) and (b) it can be seen that the MFS, in conjunction with the first-order Tikhonov regularization method and the L-curve criterion, provides accurate numerical solutions with respect to increasing the number of source points, M, with the mention that even with a small number of source points a high accuracy of the numerical displacements and tractions is achieved.

Next, we analyse the accuracy of the numerical method proposed with respect to the position of

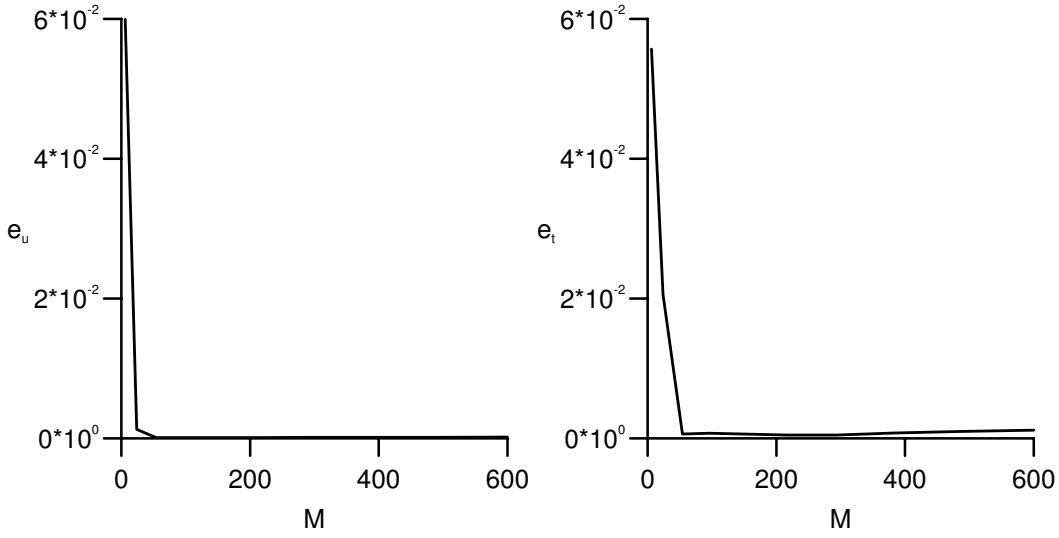

Figure 3: The accuracy errors (a) e_u and (b) e_t, obtained with $N = 500$ boundary collocation points, $R = 10.0$, $\lambda = \lambda_{\text{opt}}$ and $p_u = 5\%$ for Example 2, as functions of the number M of source points.

the source points. To do so, we set $M = 600$ and $p_u = 5$ for the Cauchy problem given by Example 2, while at the same time varying the length R. Figures 4(a) and (b) illustrate the accuracy errors e_u and e_t, respectively, as functions of R, obtained using the optimal values of $\lambda = \lambda_{\text{opt}}$ given by the L-curve criterion for each value of R. From these figures it can be seen that the larger the distance from the source points to the boundary Γ of the solution domain Ω, i.e. the larger R, the better the accuracy in the numerical displacements and tractions. It should be noted that the value $R = 2.0$ was found to be sufficiently large such that any further increase of the distance between the source points and the boundary Γ did not significantly improve the accuracy of the numerical solutions for Example 2. However, the optimal choice of R still remains an open problem, as pointed out by Katsurada and Okamoto [10], and it requires further research.

6. CONCLUSIONS

In this paper, the Cauchy problem in two- and three-dimensional isotropic linear elasticity has been investigated by employing the MFS. The resulting ill-conditioned system of linear algebraic equations has been regularized by using the first-order Tikhonov regularization method, while the choice of the optimal regularization parameter was based on the L-curve criterion. Two benchmark examples involving a

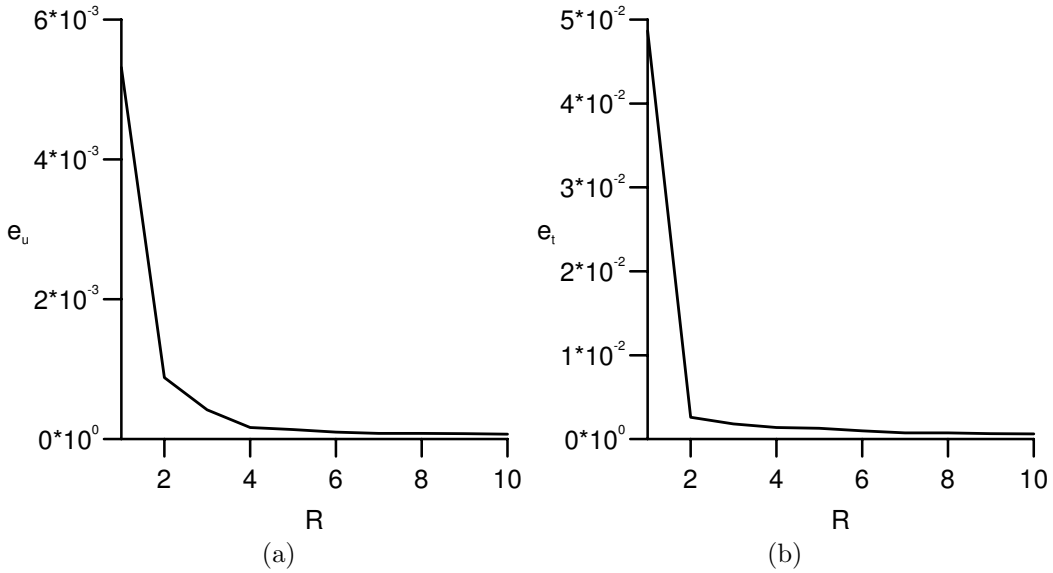

(a) (b)

Figure 4: The accuracy errors (a) e_u and (b) e_t obtained with $M = 600$ source points, $N = 500$ boundary collocation points, $\lambda = \lambda_{\text{opt}}$ and $p_u = 5\%$ for Example 2, as functions of the distance R between the source points and the boundary Γ of the solution domain Ω.

smooth two-dimensional domain and a piecewise smooth three-dimensional geometry have been analysed. The numerical results obtained show that the proposed method is convergent with respect to increasing the number of source points and the distance from the source points to the boundary of the solution domain and stable with respect to decreasing the amount of noise added into the input data. Moreover, the method is efficient, easy to adapt to irregular domains and stress concentration problems, but these investigations are deferred to future work.

REFERENCES

1. J.A. Berger and A. Karageorghis, The method of fundamental solutions for layered elastic materials. *Engng. Anal. Boundary Elem.* (2001) **25**, 877 – 886.

2. A. Bogomolny, Fundamental solutions method for elliptic boundary value problems. *SIAM J. Numer. Anal.* (1985) **22**, 644 – 669.

3. G. Fairweather and A. Karageorghis, The method of fundamental solutions for elliptic boundary value problems. *Adv. Comput. Math.* (1998) **9**, 69 – 95.

4. M.A. Golberg and C.S. Chen, The method of fundamental solutions for potential, Helmholtz and diffusion problems, *Boundary Integral Methods: Numerical and Mathematical Aspects*, (ed. M.A. Golberg), WIT Press and Computational Mechanics Publications, Boston, 1999, pp.105 – 176.

5. J. Hadamard, *Lectures on Cauchy Problem in Linear Partial Differential Equations*, Oxford University Press, London, 1923.

6. M. Hanke, Limitations of the L-curve method in ill-posed problems. *BIT* (1996) **36**, 287 – 301.

7. P.C. Hansen, *Rank-Deficient and Discrete Ill-Posed Problems: Numerical Aspects of Linear Inversion*, SIAM, Philadelphia, 1998.

8. P.C. Hansen, The L-curve and its use in the numerical treatment of inverse problems, *Computational Inverse Problems in Electrocardiology*, (ed. P. Johnston), WIT Press, Southampton, UK, 2001, pp.119 – 142.

9. C.H. Huang and W.Y. Shih, A boundary element based solution of an inverse elasticity problem by conjugate gradient and regularization method, *Proc. 7th Int. Offshore Polar Engng. Conf.*, Honolulu, USA, 1997, pp.338 – 395.

10. M. Katsurada and H. Okamoto, The collocation points of the fundamental solution method for the potential problem. *Comput. Math. Appl.* (1996) **31**, 123 – 137.

11. R.J. Knops and L.E. Payne, *Uniqueness Theorems in Linear Elasticity*, Pergamon Press, Oxford, 1986.

12. T. Koya, W.C. Yeih and T. Mura, An inverse problem in elasticity with partially overspecified boundary conditions. II. Numerical details. *Trans. ASME J. Appl. Mech.* (1993) **60**, 601 – 606.

13. V.D. Kupradze and M.A. Aleksidze, The method of functional equations for the approximate solution of certain boundary value problems. *USSR Comput. Math. Math. Phys.* (1964) **4**, 82 – 126.

14. L.D. Landau and E.M. Lifshits, *Theory of Elasticity*, Pergamon Press, Oxford, 1986.

15. A. Maniatty, N. Zabaras, and K. Stelson, Finite element analysis of some elasticity problems. *J. Engng. Mech. Division ASCE* (1989) **115**, 1302 – 1316.

16. L. Marin, L. Elliott, D.B. Ingham and D. Lesnic, Boundary element method for the Cauchy problem in linear elasticity. *Engng. Anal. Boundary Elem.* (2001) **25**, 783 – 793.

17. L. Marin, L. Elliott, D.B. Ingham and D. Lesnic, An alternating boundary element algorithm for a singular Cauchy problem in linear elasticity. *Comput. Mech.* (2002) **28**, 479 – 488.

18. L. Marin, D.N. Háo and D. Lesnic, Conjugate gradient-boundary element method for the Cauchy problem in elasticity. *Q. Jl. Mech. Appl. Math.* (2002) **55**, 227 – 247.

19. L. Marin and D. Lesnic, Regularized boundary element solution for an inverse boundary value problem in linear elasticity. *Commun. Numer. Meth. Engng.* (2002) **18**, 817 – 825.

20. L. Marin and D. Lesnic, Boundary element solution for the Cauchy problem in linear elasticity using singular value decomposition. *Comput. Meth. Appl. Mech. Engng.* (2002) **191**, 3257 – 3270.

21. R. Mathon and R.L. Johnston, The approximate solution of elliptic boundary value problems by fundamental solutions. *SIAM J. Numer. Anal.* (1977) **14**, 638 – 650.

22. A. Poullikkas, A. Karageorghis and G. Georgiou, The numerical solution for three-dimensional elastostatics problems. *Comput. Struct.* (2002) **80**, 365 – 370.

23. D. Schnur and N. Zabaras, Finite element solution of two-dimensional elastic problems using spatial smoothing. *Int. J. Numer. Meth. Engng.* (1990) **30**, 57 – 75.

21. A.N. Tikhonov and V.Y. Arsenin, *Methods for Solving Ill-Posed Problems*, Nauka, Moscow, 1986.

22. A.N. Tikhonov, A.S. Leonov and A.G. Yagola, *Nonlinear Ill-Posed Problems*, Chapman & Hall, London, 1998.

23. C.R. Vogel, Non-convergence of the L-curve regularization parameter selection method. *Inverse Problems* (1996) **12**, 535 – 547.

24. W.C. Yeih, T. Koya and T. Mura, An inverse problem in elasticity with partially overspecified boundary conditions. I. Theoretical approach. *Trans. ASME J. Appl. Mech.* (1993) **60**, 595 – 600.

28. N. Zabaras, V. Morellas and D. Schnur, Spatially regularized solution of inverse elasticity problems using the BEM. *Commun. Appl. Numer. Meth.* (1989) **5**, 547 – 553.